DOI: 10.1002/ejic.200600715

Host–Guest Complexes of Oligopyridine Cryptands: Prediction of Ion Selectivity by Quantum Chemical Calculations[‡]

Ralph Puchta*[a,b] and Rudi van Eldik[b]

Keywords: Density functional calculations / Semiempirical calculations / Cryptands / Host–guest systems / Cation selectivity

The structures and complex-formation energies for the cryptands 6,6′,6′′,6′′′,6′′′′,6′′′′′-bis[nitrilotri(methylene)]tris(2,2′-bipyridine) (**1**) and 2,2′,2′′,9,9′,9′′-bis[nitrilotri(methylene)]tris(1,10-phenanthroline) (**2**) with alkali and alkaline-earth cations are obtained by PM3/SPASS and density functional (B3LYP/LANL2DZp) calculations and the results used to predict the ion selectivity. Both cryptands **1** and **2** have a cavity size similar to [2.2.2] and prefer Ca^{2+} and Sr^{2+}, while **1** has a preference for K^+ and **2** favours Na^+ and K^+. The cryptand flexibility for **1** is attributed mainly to the bipyridine building block and that for **2** to the groups neighbouring the bridgehead nitrogen atoms.

Introduction

The selective complexation of guest molecules and ions is an essential prerequisite for the proper functioning of enzymes and receptors in biological and technical systems, and it has therefore been investigated over several decades.[1,2] In order to mimic the geometric and electronic requirements necessary for selective complexation as observed in nature, many different model compounds with cavities of variable size and structure have been studied experimentally and computationally.[3–5] Examples are the well-known calixarenes,[6,7] crown ethers,[8] cryptands,[9,10] and their inclusion complexes, along with the corresponding metallatopomers, which are easily accessible by self-organisation.[11]

The synthesis of 4,7,13,16,21,24-hexaoxa-1,10-diazabicyclo[8.8.8]hexacosane, which was reported by Dietrich, Lehn and Sauvage in 1969, today well known as [2.2.2] and traded as Kryptofix 222, led to a wide range of applications, although other cryptands with similar topology have hardly been explored. It was immediately recognized that [2.2.2] and its derivatives have an outstanding potential to selectively bind guests, in particular alkali and alkaline-earth metal ions. Today, cryptands and cryptates like [2.2.2] and their different derivatives are widely applied, for example in phase-transfer catalysis,[12,13] studies on Zintl phases,[14] selective complexation of radioactive or toxic ions in medicine[15] and elsewhere,[16,17] as chelates for MRI contrast agents,[18] and as models for carrier-antibiotics such as Valinomycin and enzyme inhibitors.[19] In contrast, the cryptands 6,6′,6′′,6′′′,6′′′′,6′′′′′-bis[nitrilotri(methylene)]tris-(2,2′-bipyridine) (**1**) and 2,2′,2′′,9,9′,9′′-bis[nitrilotri(methylene)]tris(1,10-phenanthroline) (**2**) are systems that have only been partially investigated (see Figure 1).

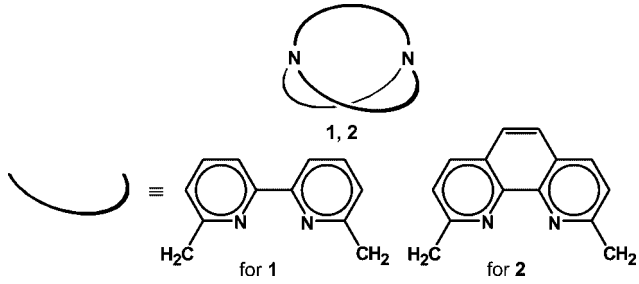

Figure 1. 6,6′,6′′,6′′′,6′′′′,6′′′′′-Bis[nitrilotri(methylene)]tris(2,2′-bipyridine) (**1**) and 2,2′,2′′,9,9′,9′′-bis[nitrilotri(methylene)]-tris(1,10-phenanthroline) (**2**).

In the 1984 report on the first synthesis of cryptands, two project aims for these newly designed polypyridine cryptands were expressed: (i) as ligand systems with novel metal-ion binding properties and (ii) special photophysical/photochemical properties for electron-transfer processes.[20] In the following years much research has been focused on their photophysics and photochemistry,[21] and the lanthanide complexes $[Ln\subset\mathbf{1}]^{3+}$ and $[Ln\subset\mathbf{2}]^{3+}$ were found to be efficient luminophores for converting UV light into visible light.[22,23] These properties can be utilized in fluorescent markers,[24] for example for detecting or locating nucleic acids,[25] or in other labelling techniques.[26] With the help of NMR techniques, the water exchange of $[Gd(H_2O)_3\subset\mathbf{1}]^{3+}$ has been investigated by Merbach et al., who tested $[Gd(H_2O)_3\subset\mathbf{1}]^{3+}$ as a potential contrast agent for magnetic

[‡] Part II; for part I see ref.[38]

[a] Computer Chemistry Center, University of Erlangen-Nürnberg, Nägelsbachstrasse 25, 91052 Erlangen, Germany
E-mail: ralph.puchta@chemie.uni-erlangen.de
[b] Institute for Inorganic Chemistry, University of Erlangen-Nürnberg,
Egerlandstrasse 1, 91058 Erlangen, Germany

resonance imaging.[27] However, for the first proposed aim and application involving the selective ion binding of **1** and **2**, only two studies on the separation of Am^{3+} and Eu^{3+} have appeared.[28,29] This is surprising since different cryptand/cryptate or crown ether-solvent combinations have been investigated,[30–34] especially with respect to their transport properties[35] or ion conductivity and potential applications in batteries and capacitors,[36] while parallel alkali and alkaline-earth ion complexes with phenanthroline and bipyridine moieties have also been studied.[37]

In a recent report we demonstrated that ion selectivity can be studied by quantum chemical methods for [2.2.2] and smaller homologues. The calculated complex-formation energy is a reliable value to conclude which ion fits best.[38] In this study we will tie up with the first report by Lehn et al., where **1** and **2** were synthesised as $[Na\subset\mathbf{1}]^+$ and $[Na\subset\mathbf{2}]^+$ (see Figures 2 and 3).[20] We have calculated the complex-formation energies for the alkali and alkaline-earth metal ions to determine which ions fit best into **1** and **2**. In addition, we have investigated how the host responds to the different guest ions.

Quantum Chemical Methods

We performed B3LYP/LANL2DZp hybrid density functional calculations, with pseudo-potentials on the heavy elements and the valence basis set augmented with polarisation functions.[39,40] During the optimisation of the structures no constraints other than symmetry were applied. In addition, the resulting structures were characterised as minima, transition structures, etc., by computation of their vibrational frequencies. The relative energies were corrected for zero-point vibrational energies (ZPE). The Gaussian suite of programs was used for all calculations.[41]

Semiempirical PM3 calculations[42] for Li^+[43], K^+[44] and Ca^{2+}[45] were performed using VAMP.[46] The PM3/

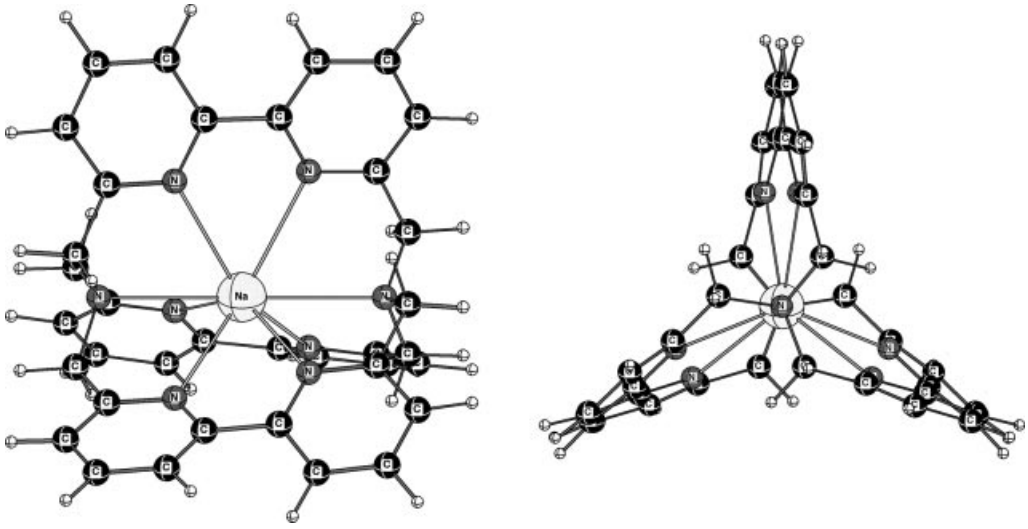

Figure 2. Calculated (RB3LYP/LANL2DZp) structure (D_3) of $[Na\subset\mathbf{1}]^+$.

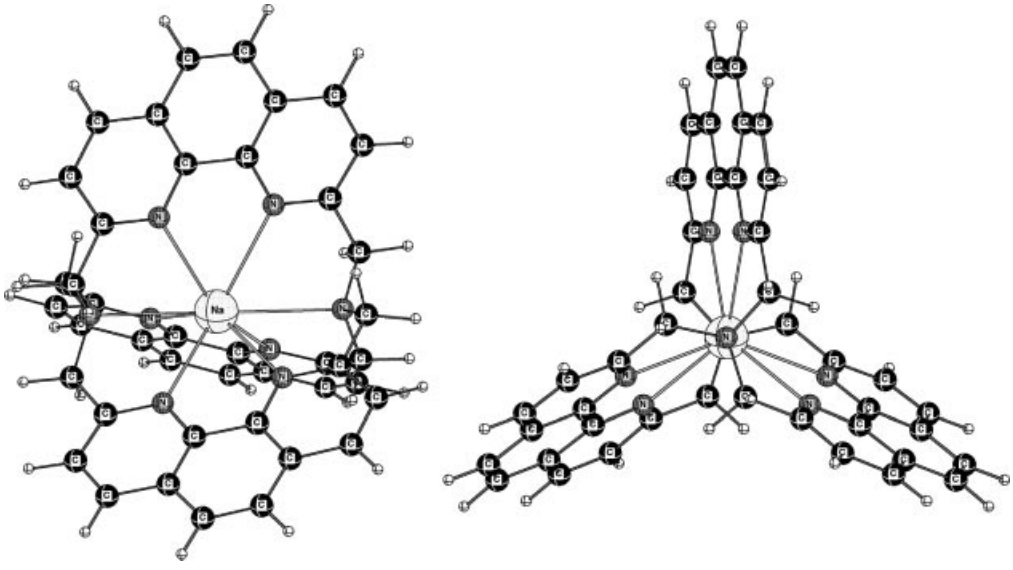

Figure 3. Calculated (RB3LYP/LANL2DZp) (D_3) and X-ray structure of $[Na\subset\mathbf{2}]^+$ (X-ray: $Na–N_{sp^2}$ = 2.70, $Na–N_{sp^3}$ = 2.79 Å[50]).

SPASS[38,47] calculations for all other alkali and alkaline-earth ions not included in PM3 were performed using MOPAC 6.0.[48]

Results and Discussion

In contrast to [2.2.2], for which X-ray structures of all alkali and alkaline-earth metal cryptate complexes have been published, only the structures of [Na **1**]$^+$e$^-$[49] and [Na⊂**2**]Br[50] have been published for **1** and **2**. The cryptatium species [Na⊂**1**]$^+$e$^-$ is an electride[49] and therefore cannot be taken into consideration. The structural parameters for the calculated (Table 2) and published X-ray structure of [Na⊂**2**]$^+$ are in satisfactory agreement (the mean X-ray bond length between Na and the sp^2-hybridized pyridine nitrogen (Na–N_{sp^2}) is 2.70 Å, and that between Na and the amine nitrogen (N_{sp^3}) is 2.79 Å),[50] as expected. Further selected data for the calculated structures (metal–N_{sp^2} and metal–N_{sp^3} distances and the twist angle) are summarised in Tables 1 and 2.

The Li^+ and Be^{2+} ions seem to be too small for **1** and **2** as the calculated D_3 structures of [Li⊂**1**]$^+$ and [Li⊂**2**]$^+$ as well as [Be⊂**1**]$^{2+}$ and [Be⊂**1**]$^{2+}$ are not local minima on the potential hypersurface. The D_3 structures of all endohedral complexed Li^+ and Be^{2+} are transition states for the movement of the metal ion inside the cavity of **1** and **2**. This motion leads from one N_{sp^3} to the other. Whereas [Li⊂**1**]$^+$ shows a clear barrier of 3.3 kcal mol^{-1} for this movement, the C_3 and D_3 conformers of [Li⊂**2**]$^+$ have no barrier, indeed D_3 is even slightly negative (–0.1 kcal mol^{-1}). The Be^{2+} ion is significantly smaller than Li^+ and therefore the barriers are higher: [Be⊂**1**]$^{2+}$ 22.4 kcal mol^{-1} and [Be⊂**2**]$^{2+}$

Table 1. Distances [Å] and angles [°] of the metal–donor interactions in **1** (calculated structures: D_3 symmetry).[a]

	Li^+ (C3)	Li^+ (t.s.)	Na^+	K^+	Rb^+	Cs^+	Be^{2+} (C3)	Be^{2+} (t.s.)	Mg^{2+}	Ca^{2+}	Sr^{2+}	Ba^{2+}
M–N_{sp^2} (DFT)	2.45/ 2.91	2.65	2.82	2.90	2.96	3.04	1.78/ 3.54	2.09	2.47	2.71	2.82	2.91
M–N_{sp^2} (PM3/SPASS)	2.54/ 2.53	–	2.79	2.78	2.86	2.88	1.71/ 4.15	–	1.89/ 4.15(C3)	2.67	2.69	2.81
M–N_{sp^3} (DFT)	2.35/ 5.15	2.81	2.82	2.94	3.01	3.09	1.76/ 5.07	3.26	2.82	2.75	2.82	2.93
M–N_{sp^3} (PM3/SPASS)	3.04/ 3.01	–	2.89	2.85	2.99	3.02	1.69/ 6.33	–	1.83/ 6.18(C3)	2.78	2.88	2.95
N_{sp^2}–C···C–N_{sp^2} (DFT)	–26.1	–23.4	21.5	34.0	41.3	54.4	–68.2	–32.7	–24.4	–14.2	15.06	26.4
N_{sp^2}–C···C–N_{sp^2} (PM3/SPASS)	–21.3	–	8.3	6.9	16.6	23.4	–100.9	–	–88.1(C3)	–8.7	–6.9	9.2
CH_2–N_{sp^3}···N_{sp^3}–CH_2 (DFT)	–99.4	–100.3	–78.4	–62.1	–53.3	–42.7	–109.0	–138.3	–113.9	–95.5	–78.2	–61.9
CH_2–N_{sp^3}···N_{sp^3}–CH_2 (PM3/SPASS)	–100.0	–	–82.5	–86.6	–67.9	–63.3	–50.3	–	–32.1(C3)	–100.8	–90.3	–73.7

[a] C3: the cryptate complex has only C_3 symmetry; t.s.: transition state.

Table 2. Distances [Å] and angles [°] of the metal–donor interactions in **2** (calculated structures: D_3 symmetry).[a]

	Li^+ (C3)	Li^+ (t.s.)	Na^+	K^+	Rb^+	Cs^+	Be^{2+} (C3)	Be^{2+} (t.s.)	Mg^{2+}	Ca^{2+}	Sr^{2+}	Ba^{2+}
M–N_{sp^2} (DFT)	2.60/ 2.91	2.69	2.75	2.84	2.90	2.97	1.92/ 3.16	2.11	2.51	2.71	2.78	2.87
M–N_{sp^2} (PM3/SPASS)	2.61/ 2.62	–	2.75	2.78	2.83	2.85	1.78/ 3.49	–	1.93/ 3.60 (C3)	2.67	2.69	2.77
M–N_{sp^3} (DFT)	2.41/ 3.25	2.82	2.84	2.90	2.96	3.03	1.79/ 4.28	3.22	2.78	2.80	2.85	2.92
M–N_{sp^3} (PM3/SPASS)	2.96/ 2.94	–	2.93	2.85	2.98	3.00	1.70/ 5.32	–	1.84/ 5.27 (C3)	2.82	2.92	2.96
N_{sp^2}–C···C–N_{sp^2} (DFT)	–2.1	–2.1	–0.2	2.8	5.1	7.7	–16.7	–16.2	–7.2	–1.6	0.4	3.0
N_{sp^2}–C···C–N_{sp^2} (PM3/SPASS)	–4.8	–	0.3	1.2	3.5	4.4	–22.4	–	–16.3(C3)	–2.2	–2.2	0.6
CH_2–N_{sp^3}···N_{sp^3}–CH_2 (DFT)	–86.8	–92.3	–85.4	–73.8	–64.9	–55.1	–119.5	–138.3	–109.9	–89.6	–80.5	–68.8
CH_2–N_{sp^3}···N_{sp^3}–CH_2 (PM3/SPASS)	–95.7	–	–83.8	–85.3	–72.4	–68.9	–122.6	–	–110.2 (C3)	–97.8	–87.5	–77.1

[a] C3: the cryptate complex has only C_3 symmetry; t.s.: transition state.

11.6 kcal mol^{-1}. The lower barriers in both cryptates based on **2** can be attributed to the rigidity of the phenanthroline moieties.

Interestingly, the quality of the structures calculated applying the simple PM3/SPASS method, in which the metal cation is modelled by a "sparkle" (a charged pseudo-atom), is very satisfactory, although the metal–sp^2-nitrogen distances are somewhat too short and the metal–sp^3-nitrogen interactions are somewhat too long compared to the DFT data.

The main goal of this work was to investigate the selective complexation of alkali and alkaline-earth metal ions by the cryptands **1** and **2**. As demonstrated in our earlier contributions,[11d,38] one can inspect two properties in order to predict whether or not an ion will be complexed. The bond length between the metal ion and the donor atoms in the cryptate can be compared with those computed for a metal ion complexed by solvent molecules like acetonitrile or ammonia. This method only seems to be of value if the donor atoms coordinating to the metal ions are the same in the cryptand and have the same hybridisation as in the solvent, and was therefore not followed further in this work. Alternatively, the energy of the model reactions shown in Equations (1) and (2) can be evaluated. Note that, for the sake of consistency, sixfold coordination is adopted for all cations. The lithium[51] and sodium cations prefer four- and fivefold coordination, respectively, with additional water molecules hydrogen-bonded in the second coordination sphere instead of being coordinated to the cation. However, in the gas phase $[Li(OH_2)_6]^+$ and $[Na(OH_2)_6]^+$ are local minima.

$$[M(H_2O)_6]^{n+} + \mathbf{1} \rightarrow [M\subset\mathbf{1}]^{n+} + 6H_2O \quad (1)$$

$$[M(H_2O)_6]^{n+} + \mathbf{2} \rightarrow [M\subset\mathbf{2}]^{n+} + 6H_2O \quad (2)$$

The complexation energies computed in this way are plotted against the ionic radii in Figures 4, 5, 6 and 7. The most stable endohedral complexes of **1** with the alkali-metal ions are formed for K^+ followed by Na^+ and with the alkaline-earth ions Ca^{2+} and Sr^{2+}, followed by Ba^{2+}. Cryptand **2** prefers to bind Na^+ followed by K^+ of the alkali-metal ions, and Ca^{2+} and Sr^{2+} followed by Ba^{2+} of the alkaline-earth ions. Therefore, we conclude that the cavity sizes of **1** and **2** are of the same order as the cavity size of [2.2.2], and that the cavity of **1** is slightly larger than that of **2**.

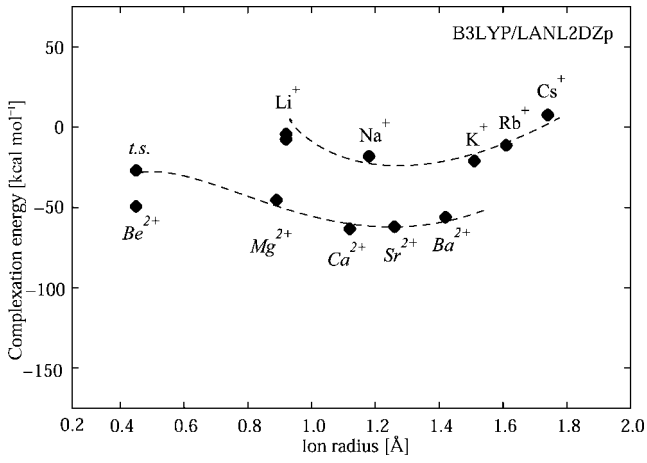

Figure 4. RB3LYP/LANL2DZp complexation energies for $[M\subset\mathbf{1}]^{n+}$ according to reaction (1), plotted against the ionic radius of M^{n+} (dashed line represents observed trend; for the data see Table 3).

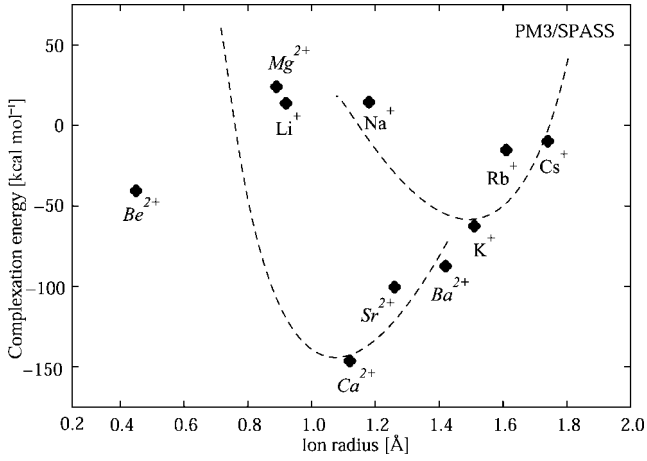

Figure 5. PM3/SPASS complexation energies for $[M\subset\mathbf{1}]^{n+}$ according to reaction (1), plotted against the ionic radius of M^{n+} (dashed line represents observed trend; for the data see Table 4).

Table 3. Energy contributions[a] to the complexation energy for $[M\subset\mathbf{1}]^{n+}$ (RB3LYP/LANL2DZp).[b]

	Li^+ (C3)	Li^+ (t.s.)	Na^+	K^+	Rb^+	Cs^+	Be^{2+} (C3)	Be^{2+} (t.s.)	Mg^{2+}	Ca^{2+}	Sr^{2+}	Ba^{2+}
ΔE_{tot}	–3.0	–2.7	–16.3	–15.2	–1.4	23.0	–23.1	–10.1	–38.0	–60.2	–60.1	–52.4
ΔZPE	–5.9	–6.3	–5.0	–5.2	–5.2	–5.1	–10.8	–12.2	–9.6	–8.5	–8.1	–6.9
Complexation energy	–8.9	–9.0	–21.2	–20.4	–6.6	17.9	–33.9	–22.3	–47.7	–68.8	–68.2	–59.4

[a] In kcal mol^{-1}. [b] C3: the cryptate complex has only C_3 symmetry; t.s.: transition state.

Table 4. Complexation energy [kcal mol^{-1}] for $[M\subset\mathbf{1}]^{n+}$ (PM3/SPASS).[a]

	Li^+ (C3)	Na^+	K^+	Rb^+	Cs^+	Be^{2+} (C3)	Mg^{2+}	Ca^{2+}	Sr^{2+}	Ba^{2+}
Complexation energy	–2.5	–8.2	–40.8	4.4	12.5	19.7	73.3	–125.9	–822	–69.4

[a] C3: the cryptate complex has only C_3 symmetry.

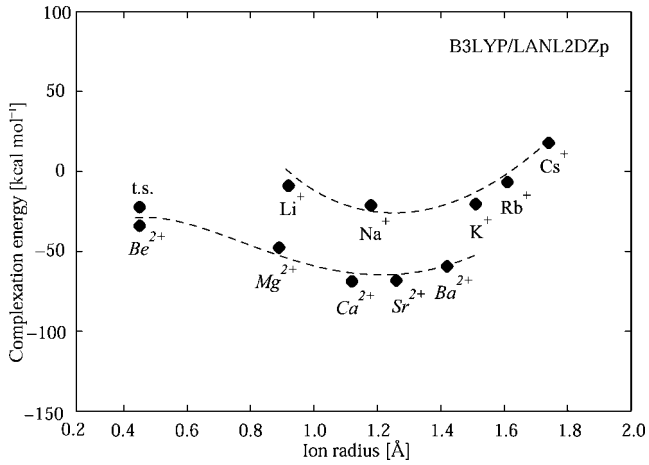

Figure 6. RB3LYP/LANL2DZp complexation energies for $[M\subset\mathbf{2}]^{n+}$ according to reaction (2), plotted against the ionic radius of M^{n+} (dashed line represents observed trend; for the data see Table 5).

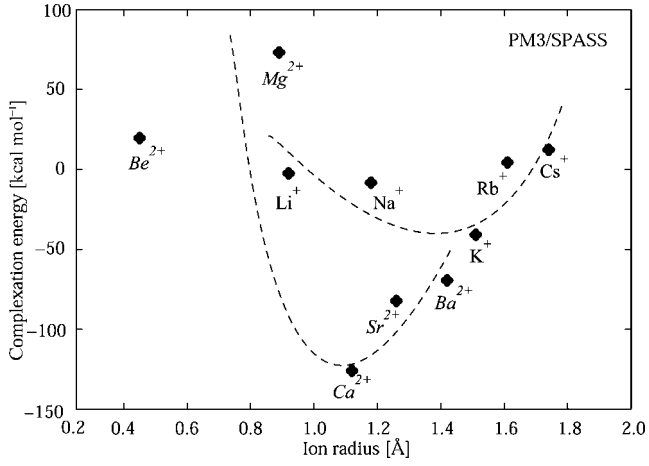

Figure 7. PM3/SPASS complexation energies for $[M\subset\mathbf{2}]^{n+}$ according to reaction (2), plotted against the ionic radius of M^{n+} (dashed line represents observed trend; for the data see Table 6).

The same trend can be qualitatively found by application of semiempirical methods, in this case PM3/SPASS. (see Figures 5 and 7) In the semiempirical series, $[Ca\subset\mathbf{1}]^{2+}$ and $[Ca\subset\mathbf{2}]^{2+}$ and, to a lesser extent, $[K\subset\mathbf{2}]^{+}$ and $[K\subset\mathbf{2}]^{+}$, are computed to be too stable. Previous studies on the endohedral complexation of Ca^{2+}[38] and calculations on $[Ca(H_2O)_n]^{2+}$ and $[Ca(NH_3)_n]^{2+}$ confirm that the calcium PM3 parameters do not describe Ca–N and Ca–O interactions correctly. The semiempirical structures of $[Mg\subset\mathbf{1}]^{2+}$ and $[Mg\subset\mathbf{2}]^{2+}$ lead to a clear fourfold-coordinated C_3 structure and therefore show a larger energy gap than in the DFT case, although the qualitative result is not affected.

A comparison of the M–N distances (Tables 1 and 2) shows an increase in the metal–donor bond lengths with increasing size of the guest ion. This behaviour is clearly attributed to the different contributions of the guest ions, but it is also a distinct hint that the investigated cryptands show some flexibility. An essential prerequisite for flexibility is that the molecular moieties can undergo twisting and tilting. While in $[M\subset\mathbf{1}]^{n+}$ every molecular bar has two N–CH_2(pyridine) motifs adjacent to the N bridgehead and a conformationally nearly unhampered C–C bond bridging the two pyridine rings, $[M\subset\mathbf{2}]^{n+}$ has only two such pyridine motifs adjacent to the N bridgehead, and the two pyridine rings in phenanthroline are stiffened by a third, weaker aromatic[52] six-membered ring. A descriptor for the twist and tilt of these moieties is the torsion angle N_{sp^2}–C···C–N_{sp^2} between the aromatic pyridine groups and the CH_2–N_{sp^3}···N_{sp^3}–CH_2 angle between the aliphatic methylene building blocks (see Tables 1 and 2).

Both sorts of torsion angles show a qualitative linear behaviour that mainly depends on the ion size (see Figures 8, 9, 10 and 11). The CH_2–N_{sp^3}···N_{sp^3}–CH_2 angle covers a wide range in both host–guest systems [96° for $[M\subset\mathbf{1}]^{n+}$ (see Figure 8)[53] and 83° for $[M\subset\mathbf{2}]^{n+}$ (see Figure 10)[53]]. Throughout the series, all cryptates show the same stereochemistry, which is easily derivable from the algebraic sign (here minus, and therefore λ). As expected, there are more drastic differences in the series of N_{sp^2}–C···C–N_{sp^2} angles. Whereas the bipyridine building block shows a 1/3 higher value for the twist (123°)[53] (see Figure 9) compared to CH_2–N_{sp^3}···N_{sp^3}–CH_2, the phenanthroline moiety is inflexible and only shows a three times lower angle (25°)[53] (see Figure 11) than CH_2–N_{sp^3}···N_{sp^3}–CH_2. Interestingly, both coordinating systems use the same principle to improve the

Table 5. Energy contributions[a] to the complexation energy for $[M\subset\mathbf{2}]^{n+}$ (RB3LYP/LANL2DZp).[b]

	Li^+ (C3)	Li^+ (t.s.)	Na^+	K^+	Rb^+	Cs^+	Be^{2+} (C3)	Be^{2+} (t.s.)	Mg^{2+}	Ca^{2+}	Sr^{2+}	Ba^{2+}
ΔE_{tot}	1.5	–1.5	–13.71	–16.59	–6.5	11.8	–38.7	–15.12	–36.2	–55.27	–54.46	–49.78
ΔZPE	–5.8	–6.1	–4.4	–4.5	–4.7	–4.2	–10.6	–11.8	–9.3	–8.1	–7.5	–6.3
Complexation energy	–4.3	–7.6	–18.1	–21.1	–11.3	7.5	–49.3	–26.9	–45.5	–63.4	–62.0	–56.1

[a] In kcal mol^{-1}. [b] C3: the cryptate complex has only C_3 symmetry; t.s.: transition state.

Table 6. Complexation energy [kcal mol^{-1}] for $[M\subset\mathbf{2}]^{n+}$ (PM3/SPASS).[a]

	Li^+ (C3)	Na^+	K^+	Rb^+	Cs^+	Be^{2+} (C3)	Mg^{2+}	Ca^{2+}	Sr^{2+}	Ba^{2+}
Complexation energy	13.8	14.4	–62.6	–15.3	–9.8	–40.6	24.0	–146.4	–100.5	–87.4

[a] C3: the cryptate complex has only C_3 symmetry.

interactions between donor and guest ion: in order to get more tilted and closer to the ion, the puckered ring formed by the pyridine moieties and guest ions interconvert their stereochemistry. Therefore, small ions like Li^+, Be^{2+} and Ca^{2+} have a λλ arrangement as both torsion angles show negative algebraic signs, whereas the larger ions K^+, Rb^+, Cs^+, Sr^{2+} and Ba^{2+} have a λδ arrangement since CH_2–N_{sp^3}···N_{sp^3}–CH_2 is negative and N_{sp^2}–C···C–N_{sp^2} is positive. The sodium cation is a special case. Thus, whereas $[Na\subset\mathbf{1}]^+$ is clearly λλ, the stiffened cryptand $[Na\subset\mathbf{2}]^+$ is only just λλ since the N_{sp^2}–C···C–N_{sp^2} angle is only –0.2°.

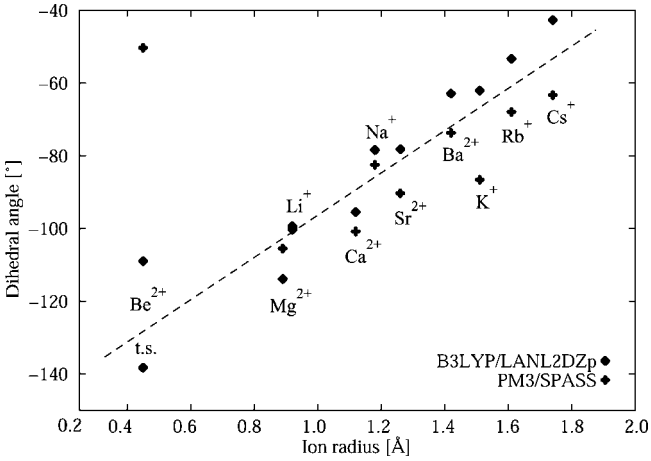

Figure 8. RB3LYP/LANL2DZp and PM3/SPASS torsion angle CH_2–N_{sp^3}···N_{sp^3}–CH_2 of $[M\subset\mathbf{1}]^{n+}$ plotted against the ionic radius of M^{n+} (dashed line represents observed trend).

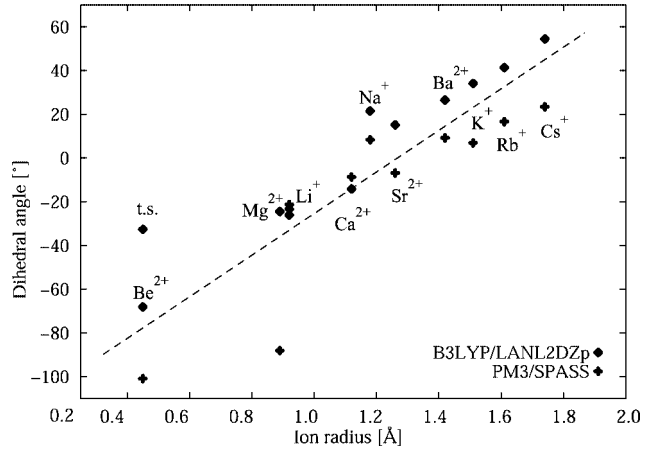

Figure 9. RB3LYP/LANL2DZp and PM3/SPASS torsion angle N_{sp^2}–C···C–N_{sp^2} of $[M\subset\mathbf{1}]^{n+}$ plotted against the ionic radius of M^{n+} (dashed line represents observed trend).

Conclusions

Density functional theory and PM3/SPASS suggest that **1** and **2** have similar-sized cavities to [2.2.2]. According to our calculations and introduced model reactions, the investigated cryptands prefer Ca^{2+} and Sr^{2+} as alkaline-earth ions, whereas K^+ is preferred by **1** and **2** binds Na^+ and K^+ equally well. The flexibility, which is important for selective

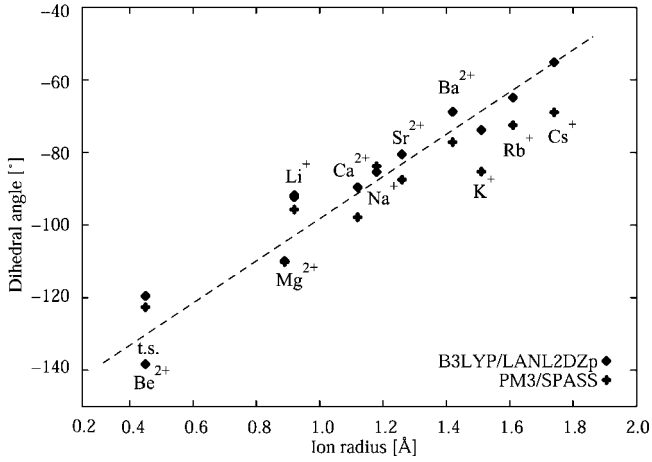

Figure 10. RB3LYP/LANL2DZp and PM3/SPASS torsion angle CH_2–N_{sp^3}···N_{sp^3}–CH_2 of $[M\subset\mathbf{2}]^{n+}$ plotted against the ionic radius of M^{n+} (dashed line represents observed trend).

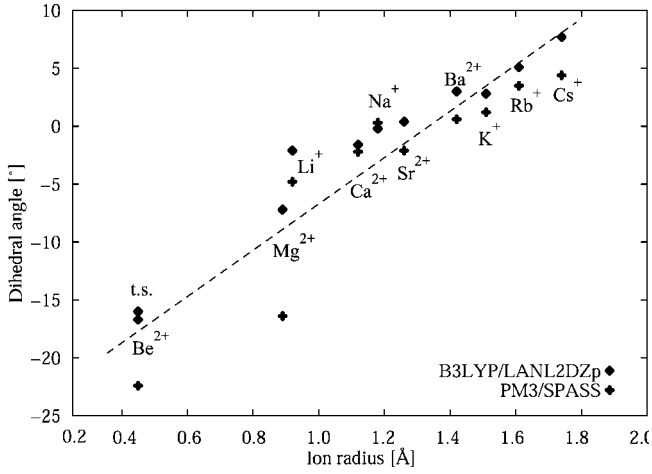

Figure 11. RB3LYP/LANL2DZp and PM3/SPASS torsion angle N_{sp^2}–C···C–N_{sp^2} of $[M\subset\mathbf{2}]^{n+}$ plotted against the ionic radius of M^{n+} (dashed line represents observed trend).

host binding, is dominated in **1** by the flexibility of the pyridine–pyridine connection, whereas in the more rigid **2** the CH_2–N_{sp^3}···N_{sp^3}–CH_2 motif contributes the main part. The stereo-arrangement of the molecular cage axis fixed at the bridgehead nitrogen is identical in all host–guest systems investigated and does not change during the calculations. On the contrary, the stereochemistry of the coordinating bipyridine and phenanthroline moieties can change depending on the size of the guest ion.

Acknowledgments

The authors gratefully acknowledge financial support from the Deutsche Forschungsgemeinschaft as part of the SFB 583 "Redox-Active Metal Complexes" and the Fonds der Chemischen Industrie. We thank Prof. Tim Clark for hosting this work at the CCC, Nico van Eikema Hommes and Roland Meier for helpful discussions, and the Regionales Rechenzentrum Erlangen (RRZE) for a generous allotment of computer time.

[1] F. Haber, *Angew. Chem.* **1927**, *40*, 303–314.
[2] E. Bayer, H. Fiedler, K.-L. Hock, D. Otterbach, G. Schenk, W. Voelter, *Angew. Chem.* **1964**, *76*, 76–83; *Angew. Chem. Int. Ed. Engl.* **1964**, *3*, 325–332 and the literature cited therein.
[3] J.-M. Lehn, *Supramolecular Chemistry*, VCH, Weinheim **1995**.
[4] F. Vögtle, *Supramolekulare Chemie*, Teubner, Stuttgart **1992**.
[5] G. Jaouen, *Bioorganometallics*, Wiley-VCH, Weinheim **2005**.
[6] See, for example: a) J. Schatz, *Collect Czech. Chem. Commun.* **2004**, *69*, 1169–1194; b) R. Puchta, T. Clark, W. Bauer, *J. Mol. Model.* **2006**, *12*, 739–747.
[7] W. Śliwa, *Pol. J. Chem.* **2001**, *75*, 921–940.
[8] See, for example, a) C. J. Pedersen, *Angew. Chem.* **1988**, *100*, 1053–1059; *Angew. Chem. Int. Ed. Engl.* **1988**, *27*, 1021–1027; b) D. J. Cram, *Angew. Chem.* **1988**, *100*, 1041–1052; *Angew. Chem. Int. Ed. Engl.* **1988**, *27*, 1009–1020; c) J.-M. Lehn, *Angew. Chem.* **1988**, *100*, 91–116; *Angew. Chem. Int. Ed. Engl.* **1988**, *27*, 89–112 and the literature cited therein; d) J. Ellermann, W. Bauer, M. Schütz, F. W. Heinemann, M. Moll, *Monatsh. Chem.* **1998**, *129*, 547–566; e) S. H. Hausner, C. A. F. Striley, J. A. Krause-Bauer, H. Zimmer, *J. Org. Chem.* **2005**, *70*, 5804–5817.
[9] See, for example: J.-M. Lehn, *Acc. Chem. Res.* **1978**, *11*, 49–57.
[10] B. Dietrich, P. Viout, J-M. Lehn, *Macrocyclic Chemistry*, VCH, Weinheim **1993**.
[11] See, for example: a) R. W. Saalfrank, A. Dresel, V. Seitz, S. Trummer, F. Hampel, M. Teichert, D. Stalke, C. Stadler, J. Daub, V. Schünemann, A. X. Trautwein, *Chem. Eur. J.* **1997**, *3*, 2058–2061; b) R. W. Saalfrank, N. Löw, S. Kareth, V. Seitz, F. Hampel, D. Stalke, M. Teichert, *Angew. Chem.* **1998**, *110*, 182–184; *Angew. Chem. Int. Ed.* **1998**, *37*, 172–174; c) R. W. Saalfrank, V. Seitz, D. L. Caulder, K. N. Raymond, M. Teichert, D. Stalke, *Eur. J. Inorg. Chem.* **1998**, 1313–1317; d) R. Puchta, V. Seitz, N. J. R. van Eikema Hommes, R. W. Saalfrank, *J. Mol. Model.* **2000**, *6*, 126–132; e) R. W. Saalfrank, V. Seitz, F. W. Heinemann, C. Göbel, R. Herbst-Irmer, *J. Chem. Soc., Dalton Trans.* **2001**, 599–603; f) R. W. Saalfrank, I. Bernt, E. Uller, F. Hampel, *Angew. Chem.* **1997**, *109*, 2596–2599; *Angew. Chem. Int. Ed. Engl.* **1997**, *36*, 2482–2485; g) O. Waldmann, J. Schülein, R. Koch, P. Müller, I. Bernt, R. W. Saalfrank, H.-P. Andres, H. U. Güdel, *Inorg. Chem.* **1999**, *38*, 5879–5886; h) R. W. Saalfrank, Ch. Deutscher, H. Maid, A. M. Ako, S. Sperner, T. Nakajima, W. Bauer, F. Hampel, B. A. Heß, N. J. R. van Eikema Hommes, R. Puchta, F. W. Heinemann, *Chem. Eur. J.* **2004**, *10*, 1899–1905; i) R. W. Saalfrank, T. Nakajima, N. Mooren, A. Scheurer, H. Maid, F. Hampel, Ch. Trieflinger, J. Daub, *Eur. J. Inorg. Chem.* **2005**, 1149–1153 and the literature cited therein.
[12] See, for example: E. V. Demlov, *Phase Transfer Catalysts*, MERCK-Schuchardt, Darmstadt.
[13] See, for example: J.-H. Li, J. S. Shih, *J. Chin. Chem. Soc.* **1999**, *46*, 885–888.
[14] See, for example: C. E. Housecroft, *Clusterverbindungen von Hauptgruppenelementen*, VCH, Weinheim, **1994**.
[15] See, for example: W. H. Müller, *Naturwissenschaften* **1970**, *57*, 248; J.-M. Lehn, F. Montavon, *Helv. Chim. Acta* **1978**, *61*, 67–82; J.-M. Lehn, M. Kirch, *Angew. Chem.* **1975**, *87*, 542–543; *Angew. Chem. Int. Ed. Engl.* **1975**, *14*, 555–556.
[16] See, for example: H. S. Ajgaonkar, S. M. Khopkar, *Chem. Anal.* **1999**, *44*, 61–66.
[17] D. Tait, G. Haase, A. Wiechen, *Kieler Milchwirtschaftliche Forschungsberichte* **1998**, *50*, 211–223.
[18] L. Burai, R. Scopelliti, E. Tóth, *Chem. Commun.* **2002**, 2366–2367.
[19] M. Farahbakhsh, H. Schmidt, D. Rehder, *Chem. Ber./Recueil* **1997**, *130*, 1123–1127.
[20] J.-C. Rodriguez-Urbi, B. Alpha, D. Plancherel, J.-M. Lehn, *Helv. Chim. Acta* **1984**, *67*, 2264–2269.
[21] H. Dürr, K. Zengerle, H. P. Trierweiler, *Z. Naturforsch. Teil B* **1988**, *43*, 361–367.
[22] B. Alpha, J.-M. Lehn, G. Mathis, *Angew. Chem.* **1987**, *99*, 259–261; *Angew. Chem. Int. Ed. Engl.* **1987**, *26*, 266–267.
[23] B. Alpha, V. Balzani, J.-M. Lehn, S. Perathoner, N. Sabbatini, *Angew. Chem.* **1987**, *99*, 1310–1311; *Angew. Chem. Int. Ed. Engl.* **1987**, *26*, 1266–1267.
[24] G. Mathis, J.-M. Lehn, FR 2570703, **1986**.
[25] H. Bazin, G. Mathis, WO 9918114, **1999**.
[26] M. A. Billadeau, J. K. Leland, L. Shen, WO 9641177, **1996**.
[27] L. Burai, E. Tóth, H. Bazin, M. Benmelouka, Z. Jászberényi, L. Helm, A. E. Merbach, *Dalton Trans.* **2006**, 629.
[28] V. K. Manchana, P. K. Mohapatra, *J. Incl. Phenom.* **1993**, *15*, 121–130.
[29] V. K. Manchana, P. K. Mohapatra, *Polyhedron* **1993**, *12*, 1115–1117.
[30] E. Karkhaneei, M. H. Zebarjadian, M. Shamsipur, *J. Solution Chem.* **2001**, *30*, 323–333.
[31] T. Madrakian, M. Shamsipur, *J. Coord. Chem.* **2000**, *52*, 139–149.
[32] M. Hojo, I. Hisatsune, H. Tsurui, S. Minami, *Anal. Sci.* **2000**, *16*, 1277–1284.
[33] T. Madrakian, M. Shamsipur, *Polyhedron* **1996**, *15*, 1681–1685.
[34] M. Shamsipur, E. Karkhaneei, A. Afkhami, *J. Coord. Chem.* **1998**, *44*, 23–32.
[35] A. D′Aprano, B. Sesta, A. Capalbi, M. Immarino, V. Mauro, *J. Electroanal. Chem.* **1996**, *403*, 257–260.
[36] E. Pasgreta, R. Puchta, M. Galle, N. J. R. van Eikema Hommes, A. Zahl, R. van Eldik, *J. Incl. Phenom.*; DOI: 10.1007/s10847-006-9125-y.
[37] T. Madrakian, A. Afkhami, J. Ghasemi, M. Shamsipur, *Polyhedron* **1996**, *15*, 3647–3652.
[38] M. Galle, R. Puchta, N. J. R. van Eikema Hommes, R. van Eldik, *Z. Phys. Chem.* **2006**, *220*, 511–523.
[39] a) A. D. Becke, *J. Phys. Chem.* **1993**, *97*, 5648–5652; b) C. Lee, W. Yang, R. G. Parr, *Phys. Rev. B* **1988**, *37*, 785–789; c) P. J. Stephens, F. J. Devlin, C. F. Chabalowski, M. J. Frisch, *J. Phys. Chem.* **1994**, *98*, 11623–11627; d) T. H. Dunning Jr, P. J. Hay, *Mod. Theor. Chem.* **1976**, *3*, 1–28; e) P. J. Hay, W. R. Wadt, *J. Chem. Phys.* **1985**, *82*, 270–283; f) P. J. Hay, W. R. Wadt, *J. Chem. Phys.* **1985**, *82*, 284–298; g) P. J. Hay, W. R. Wadt, *J. Chem. Phys.* **1985**, *82*, 299–310; h) *Gaussian Basis Sets for Molecular Calculations* (Ed.:), S. Huzinaga, Elsevier, Amsterdam **1984**.
[40] The performance of the computational level employed in this study is well documented. See for example: a) R. Puchta, R. Meier, N. J. R. van Eikema Hommes, R. van Eldik, *Eur. J. Inorg. Chem.* **2006**, 4063–4067; b) A. Scheurer, H. Maid, F. Hampel, R. W. Saalfrank, L. Toupet, P. Mosset, R. Puchta, N. J. R. van Eikema Hommes, *Eur. J. Org. Chem.* **2005**, 2566–2574; c) P. Illner, A. Zahl, R. Puchta, N. van Eikema Hommes, P. Wasserscheid, R. van Eldik, *J. Organomet. Chem.* **2005**, *690*, 3567–3576; d) Ch. F. Weber, R. Puchta, N. van Eikema Hommes, P. Wasserscheid, R. van Eldik, *Angew. Chem.* **2005**, *117*, 6187–6192; *Angew. Chem. Int. Ed.* **2005**, *44*, 6033–6038.
[41] *Gaussian 03*, Revision C.02, M. J. Frisch, G. W. Trucks, H. B. Schlegel, G. E. Scuseria, M. A. Robb, J. R. Cheeseman, J. A. Montgomery Jr, T. Vreven, K. N. Kudin, J. C. Burant, J. M. Millam, S. S. Iyengar, J. Tomasi, V. Barone, B. Mennucci, M. Cossi, G. Scalmani, N. Rega, G. A. Petersson, H. Nakatsuji, M. Hada, M. Ehara, K. Toyota, R. Fukuda, J. Hasegawa, M. Ishida, T. Nakajima, Y. Honda, O. Kitao, H. Nakai, M. Klene, X. Li, J. E. Knox, H. P. Hratchian, J. B. Cross, C. Adamo, J. Jaramillo, R. Gomperts, R. E. Stratmann, O. Yazyev, A. J. Austin, R. Cammi, C. Pomelli, J. W. Ochterski, P. Y. Ayala, K. Morokuma, G. A. Voth, P. Salvador, J. J. Dannenberg, V. G. Zakrzewski, S. Dapprich, A. D. Daniels, M. C. Strain, O. Farkas, D. K. Malick, A. D. Rabuck, K. Raghavachari, J. B. Foresman, J. V. Ortiz, Q. Cui, A. G. Baboul, S. Clifford, J. Cioslowski, B. B. Stefanov, G. Liu, A. Liashenko, P. Piskorz, I. Komaromi, R. L. Martin, D. J. Fox, T. Keith, M. A. Al-Laham, C. Y. Peng, A. Nanayakkara, M. Challacombe, P. M. W. Gill,

B. Johnson, W. Chen, M. W. Wong, C. Gonzalez, and J. A. Pople, Gaussian, Inc., Wallingford CT, **2004**.
[42] J. J. P. Stewart, *J. Comput. Chem.* **1989**, *10*, 209–220; J. J. P. Stewart, *J. Comput. Chem.* **1991**, *12*, 320–341.
[43] E. Anders, R. Koch, P. Freunscht, *J. Comput. Chem.* **1993**, *14*, 1301–1312.
[44] Z. Havlas, S. Nick, H. Bock, *Int. J. Quantum Chem.* **1992**, *44*, 449–467.
[45] J. Yu, W. J. Hehre, to be published (implemented in Spartan, Version 4.1 and higher).
[46] VAMP 7.5a, T. Clark, A. Alex, B. Beck, J. Chandrasekhar, P. Gedeck, A. Horn, M. Hutter, B. Martin, G. Rauhut, W. Sauer, T. Schindler, T. Steinke, Erlangen **1999**.
[47] PM3 augmented with a Sparkle parameter for Na^+, Rb^+, Cs^+, Sr^{2+} and Ba^{2+}, R. Puchta, PhD Thesis, Erlangen, **2003**.
[48] MOPAC 6.0: J. J. P. Stewart, *QCPE 455*.
[49] L. Echegoyen, A. DeCian, J. Fischer, J.-M. Lehn, *Angew. Chem.* **1991**, *103*, 884–886; *Angew. Chem. Int. Ed. Engl.* **1991**, *30*, 838–840.
[50] A. Caron, J. Guilhem, C. Rieche, C. Pascard, B. Alpha, J.-M. Lehn, J.-C. Rodriguez-Urbis, *Helv. Chim. Acta* **1985**, *68*, 1577–1582.
[51] R. Puchta, M. Galle, N. van Eikema Hommes, E. Pasgreta, R. van Eldik, *Inorg. Chem.* **2004**, *43*, 8227–8229 and the literature cited therein.
[52] Z. Chen, Ch. S. Wannere, C. Corminboeuf, R. Puchta, P. von Ragué Schleyer, *Chem. Rev.* **2005**, *105*, 3842–3888.
[53] Values taken from the DFT calculations.

Received: August 1, 2006
Published Online: February 9, 2007

